Creep Fracture and Grain Structure of Pure ECAP Aluminum and Copper

I. Saxl[1,2], V. Sklenička[3], L. Ilucová[1], M. Svoboda[3], P. Král[3], J. Dvořák[3]
[1]Mathematical Institute, Academy of Sciences of the Czech Republic, Žitná 25, CZ-115 67 Praha, Czech Republic; [2]Faculty of Mathematics and Physics, Charles University, Sokolovská 83, CZ-186 75, Praha, Czech Republic; [3]Institute of Physics of Materials, Academy of Sciences of the Czech Republic, Žižkova 22, CZ-616 62 Brno, Czech Republic

1. Introduction

The equal channel angular pressing (ECAP) technology seems to be the most promising one among severe plastic deformation techniques and attracts recently a great research attention [1, 2]. However, the structure produced by its application and the creep properties of the resulting materials have not been sufficiently examined as yet [3-9]. In our previous papers [10-13], the grain and subgrain structure of originally coarse-grained pure aluminum (high stacking fault energy) after ECAP and subsequent creep was examined by means of the electron backscatter diffraction (EBSD) at selected lower bounds of the misorientation Δ. The grain and subgrain structures were characterized by the mean area intensity (density) of boundaries and subboundaries per unit volume S and by the mean length intensity (density) of triple grain and subgrain junctions per unit volume L. The structural homogeneity was qualified by the coefficient of variation CV a of the profile areas. The following results were obtained:

i) The as-pressed state: whereas the overall density $S(2^o)$ observed at $\Delta \geq 2^o$ did not change substantially with the number of ECAP passes between $N = 1$ and 12, a considerable lack of true grain boundaries (with the misorientation value Δ exceeding 15^o) was observed after the low number of passes, N = 1, 2 say, and their contribution to $S(2^o)$ was lower than 10 %. With the increasing number of passes N, a considerable amount of the subgrain boundaries was gradually transformed to the true grain boundaries and their fraction at N = 12 was about 60 %. The local inhomogeneity of structure as characterized by the values of CV a as high as 10 at $N = 2$ gradually improved and the values of CV a of the order of 1 were observed at $N \geq 8$. During annealing at the creep testing temperatures (473 K, 573 K), a substantial grain and subgrain growth took place but the lack of true grain boundaries after low numbers of passes remained conserved.
ii) The time to fracture increased substantially after the first pass (much more than 100 times at certain stresses and temperatures), but quickly decreased after repeated passes (e.g. the times to fracture were approximately $t_f(N = 1) = 1000$ h and $t_f(N = 12) = 20$ h at 473 K and 15 MPa).

In the present paper the same approach was accepted in order to examine the properties of originally coarse-grained pure copper (low stacking fault energy). Some properties of copper after ECAP are similar, in particular the improvement of creep properties after small number of passes, their rapid deterioration with

increasing number of passes and a considerable grain growth on annealing. However, the development of subgrain and grain boundary structures during repeated passes and subsequent creep is completely different. In the last part of the paper, the Monkman-Grant relation between the time to fracture t_f and the minimum creep rate $\dot{\varepsilon}_{min}$ is examined and a great similarity is found between the behavior of aluminum and copper produced by ECAP technology.

2. Experimental procedures

The ECAP was carried out at room temperature with a die having the internal angle of 90° between the two parts of the channel and an outer arc of curvature of approximately 20° at the external intersection of parts. The numbers of passes at 293 K were N = 1, 2, 4, 8, 12, their sequence was performed by route B_C (the billet is rotated by 90° in the same direction after each pass); for details concerning the fabrication of the experimental materials and ECAP technique see [14, 15]. As-pressed specimens, specimens after annealing and specimens after creep testing at the temperatures 473 K and 573 K at various stress levels (between 50 and 100 MPa) were examined by means of scanning electron microscope (SEM) equipped with an electron backscatter diffraction (EBSD). Four intervals of the boundary misorientation Δ were examined: subgrain boundaries with $2^o \le \Delta < 5^o$ and $5^o \le \Delta < 10^o$, transitive subboundaries $10^o \le \Delta < 15^o$, and, conventionally defined true grain boundaries at $\Delta \ge 15^o$.

Selected results concerning copper have been already published in [16], in particular the number fractions of high angle boundaries as revealed by EBSD. In the present paper, the stereological approach is chosen, namely the area fraction of boundaries with certain misorientation and the corresponding length of triple subgrain and grain junction are estimated. In order to describe the orientation of the examined section planes w. r. to ECAP pressing, a Cartesian coordinate system was chosen with the X-axis along the last pressing direction and Z-axis perpendicular to the bottom of the channel. Three mutually perpendicular planar sections XY, XZ (longitudinal sections) and YZ (transverse section) were examined in aluminum, in copper only the transverse section XZ was observed. The standard intercept count in six systematically selected directions was carried out and the mean value N_L (the mean number per unit line of intercepts with profile boundaries) was used to estimate the density S, namely $[S] = 2N_L$ (the brackets denote the unbiased estimation). The profile count was accomplished in the section plane (in three section planes in aluminum): the mean number per unit area of profiles N_A serves to estimate the triple grain junction density, namely $[L] = 4N_A$. For a discussion concerning these stereological relations see e.g. [17].

3. Results

The as-pressed structures of copper are shown in Fig. 1. Note the vast diagonal profiles of subgrains after N = 2, 4 at $\Delta \ge 2^o$ which turn out to belong to one profile only of an extensive true grain at $\Delta \ge 15^o$ filled with very small and

frequently isolated true grains. The presence of these small precipitate-like true grains formed already during the first pass and stable during subsequent passes is a typical feature of copper structure after ECAP. The quantitative characterization of this behavior can be seen in Table 1. In contrast to aluminum, high angle boundaries strictly prevail and the fraction of subboundaries with $5^o \le \Delta < 15^o$ is low. However, for the dominant area fraction (above 60 %) of high angle boundaries are responsible small grains dispersed in the interior of very large grains. The mean grain volume is of the order of 1 μm^3, but the grain size dispersion is extremely high (see Table 5). The case of $N = 1$ is exceptional: the high angle boundaries were very scarce because of the grain profile sizes exceeding the observing window. Consequently, the mean values of S at $N = 1$ given in Table 1 perhaps underestimate the real situation.

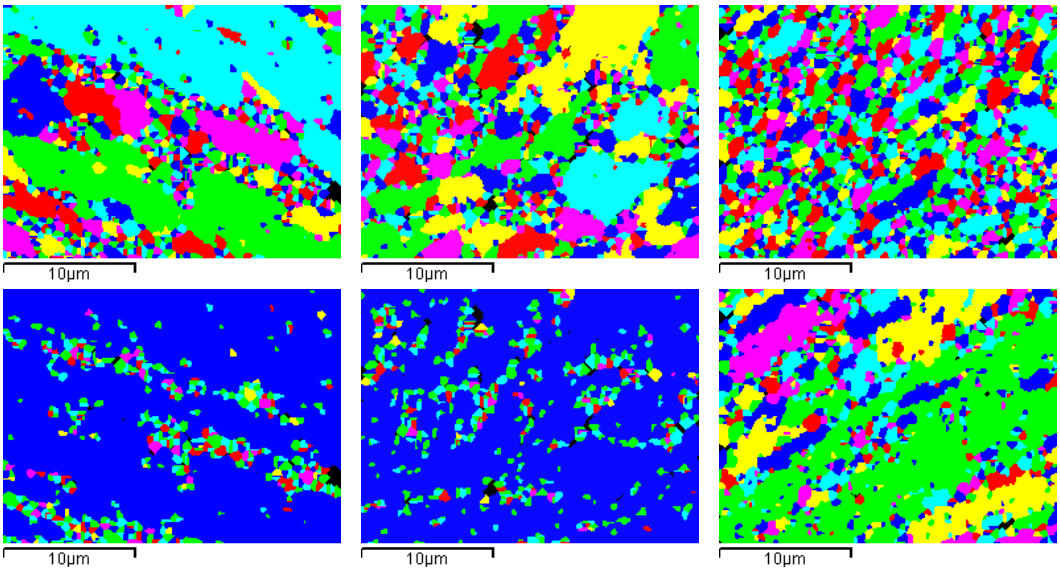

Fig. 1 EBSD images of as-pressed copper (*XZ* sections, the *X* axis is horizontal): $\Delta \ge 2^o$ (upper row), $\Delta \ge 15^o$ (lower row), $N = 2$ (left), 4 (middle), 8 (right).

Table 1 Total area intensity $S(\Delta \ge 2^o)$ of subgrain and grain boundaries and the proportional fractions of intensity $S(\Delta \ge 2^o)$ corresponding to the chosen ranges of misorientation in as-pressed specimens and in specimens after $N = 8$ passes subsequently annealed (10 and 100 hours) at two different temperatures.

	Intensity S[μm^{-1}] and its fractions (in %) in Δ-ranges of as-pressed Cu					**S[μm^{-1}] and its fractions (in %) in as-pressed Cu (N= 8), annealing time [h]**			
Δ-ranges	***N***					**473 K**		**573 K**	
	1	**2**	**4**	**8**	**12**	**10**	**100**	**10**	**100**
$[2^o, 5^o)$	63	22	27	15	-	0	7	2	14
$[5^o, 10^o)$	0	4	8	14	-	1	0	1	1
$[10^o, 15^o)$	0	2	1	5	-	1	1	1	1
$\ge 15^o$	37	72	64	66	-	98	92	96	84
$S(\Delta \ge 2^o)$	**0.350**	**2.22**	**2.80**	**3.70**	**-**	**0.96**	**0.90**	**0.68**	**0.80**

Table 1 contains also the structural characteristics of copper annealed after $N = 8$ at two different temperatures, namely 473 K and 573 K – see Fig. 2. There is no substantial qualitative difference between the obtained images: the true grain boundaries strictly prevail even after shorter annealing time at the lower temperature. Further, the subboundaries with $5^o \le \Delta < 15^o$ are nearly completely missing after annealing. The subgrain and grain profiles are more than 10 times greater, or, the mean grain width increases very approximately 5 times (see Table 3, in which the intensity L is inversely proportional to the mean profile size) thus manifesting the instability of structure with respect to annealing.

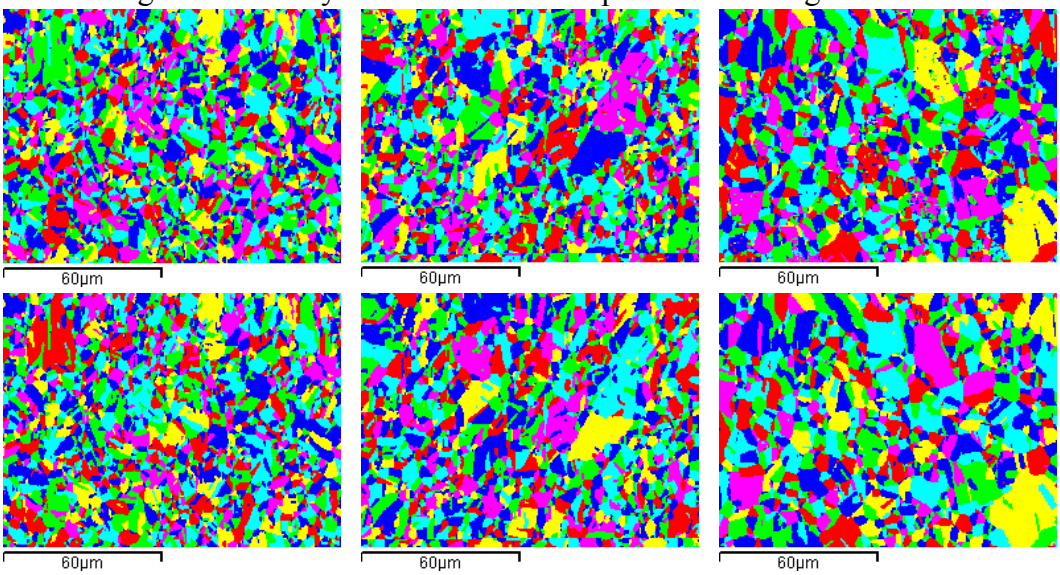

Fig. 2 *XZ* sections of as-pressed ($N = 8$) and annealed copper: 473 K, 10 h (left) and 100 h (middle), 573 K, 100 h (right), $\Delta \ge 2^o$ (upper row), $\Delta \ge 15^o$ (lower row).

Finally, we shall consider the structures after creep (Table 2, Fig. 3). The annealing times at different stresses and temperatures were substantially diverse, namely several hundred of hours at $N = 1$, 2 and stress 80 MPa at 473 K and between approx. 70 and 140 hours in the remaining cases.

Table 2 Total area intensity $S(\Delta \ge 2^o)$ of subgrain and grain boundaries and the proportional fractions of intensity $S(\Delta \ge 2^o)$ corresponding to the chosen ranges of misorientation after creep at two different temperatures and stresses.

	Intensity S [μm^{-1}] after creep and its fractions (in %) in Δ-ranges									
	473 K, 80 MPa					**573 K, 50 MPa**				
Δ-ranges	**1**	**2**	**4**	**8**	**12**	**1**	**2**	**4**	**8**	**12**
$[2^o, 5^o)$	24	7	20	14	24	2	27	19	11	15
$[5^o, 10^o)$	1	3	3	2	2	0	0	1	0	0
$[10^o, 15^o)$	8	8	1	1	1	0	0	1	1	4
$\ge 15^o$	67	82	83	83	73	98	73	79	88	81
$\boldsymbol{S(\Delta \ge 2^o)}$	**0.154**	**0.246**	**0.654**	**0.348**	**0.324**	**0.144**	**0.112**	**0.190**	**0.176**	**0.146**

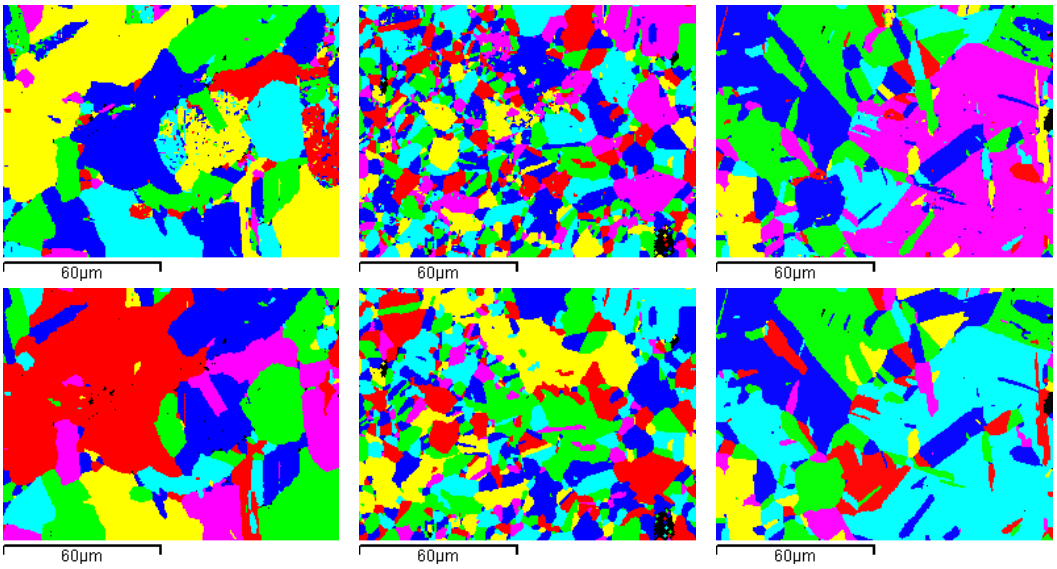

Fig. 3 *XZ* sections of copper specimens after annealing during the creep tests at 473 K and 80 MPa: $\Delta \geq 2^o$ (upper row) and $\Delta \geq 15^o$ (lower row), N = 1 (left), 4 (middle), 12 (right).

The substantial grain coarsening came up (very roughly about 10 times in the mean width at 473 K and 25 times at 573 K; see again Tables 2 and 4). However, from the qualitative point of view (subgrain and grain shapes, profile dispersion), the structures developed at the both temperatures are similar. The previously observed structural features, in particular particle-like subgrains and grains freely dispersed within larger grains can be again observed. Twins are rather frequent and were not observed in the as-pressed and annealed specimens. Table 2 again confirms the low share of subboundaries with $5^o \leq \Delta < 15^o$.

Table 3 Total length intensity L ($\Delta \geq 2^o$) of triple subgrain and grain junctions boundaries and its fractions (in %) corresponding to the chosen ranges of misorientation in as-pressed and as-pressed annealed specimens.

	Intensity L [μm^{-2}] and its fractions (in %) in Δ-ranges								
	As-pressed					**As-pressed N=8, annealing time[h]**			
Δ-ranges	***N***					**473 K**		**573 K**	
	1	**2**	**4**	**8**	**12**	**10**	**100**	**10**	**100**
$[2^o, 5^o)$	92	20	25	26	-	0	19	7	31
$[5^o, 10^o)$	0	5	6	15	-	3	1	3	18
$[10^o, 15^o)$	0	3	3	8	-	4	4	2	27
$\geq 15^o$	8	72	66	51	-	93	76	88	64
L ($\Delta \geq 2^o$)	**0.840**	**4.76**	**6.40**	**8.64**	**-**	**0.616**	**0.556**	**0.350**	**0.440**

Whereas the results concerning area density of boundaries can be considered as reliable, the estimates of length densities L are somewhat questionable. The

estimate $[L] = 4N_A$ is based on the assumption that profiles create a random tessellation in the section plane with the mean number of vertices per cell equal to 2 (the profile vertices are the traces of triple grain junctions). However, the presence of isolated grains without vertices makes this assumption invalid. Hence the length densities summarized in Tables 3 and 4 are overestimated in the specimens with isolated subgrains and grains and the dependence of L on the number of passes is questionable. The effect of the number of passes N on the intensities S and L in copper is compared with our previous results for aluminum are compared in Fig. 4. Whereas the growth of true grain fractions with N is quite distinct in aluminum, such a behavior cannot be proved for copper and the differences in S, L at individual values of N reflect rather a great scatter of results than some reasonable dependence (in particular at $N = 1$).

Table 4 Total length intensity $L(\Delta \geq 2^o)$ of triple subgrain and grain junctions and its fractions (in %) corresponding to the chosen ranges of misorientation after creep at two different temperatures.

	Intensity L[μm^{-2}] and its fractions (in %) in Δ-ranges after creep									
	473K, 80 MPa					**573K, 50 MPa**				
Δ-ranges	**1**	**2**	**4**	**8**	**12**	**1**	**2**	**4**	**8**	**12**
$[2^o, 5^o)$	65	28	43	46	54	53	77	52	30	63
$[5^o, 10^o)$	3	7	4	5	2	1	4	2	3	3
$[10^o, 15^o)$	2	3	3	4	1	2	0	1	1	2
$\geq 15^o$	30	62	50	45	43	54	19	45	66	32
$L(\Delta \geq 2^o)$	**0.069**	**0.063**	**0.344**	**0.152**	**0.184**	**0.023**	**0.021**	**0.037**	**0.038**	**0.025**

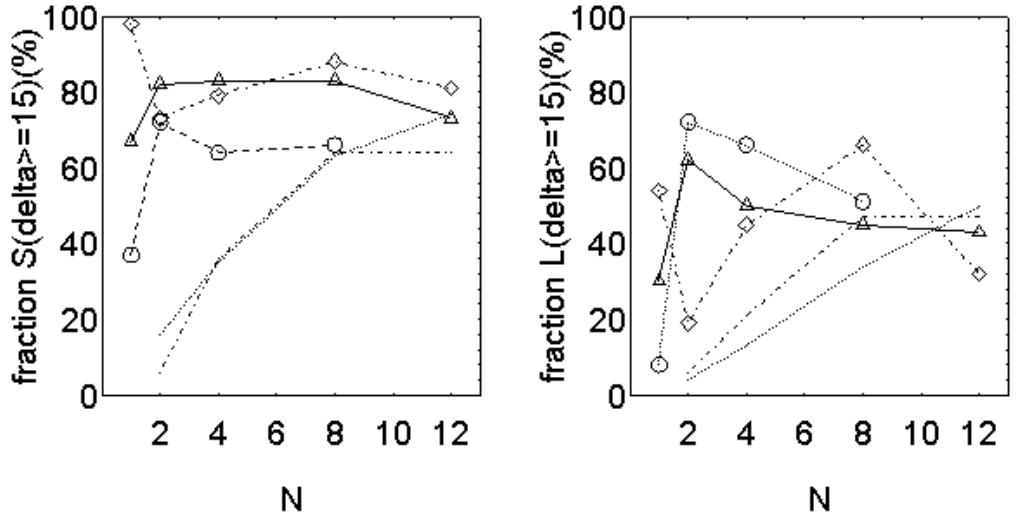

Fig. 4 Fraction of true high angle boundaries ($\Delta \geq 15^o$) for as-pressed copper (circles) and after creep at 473 K (80 MPa, triangles) and 573 K (50 MPa, squares) as compared with aluminum (as-pressed, dotted line) and after creep (473 K and 20 MPa, dash-and-dot).

The estimated values of the coefficients of variation CV *a* describing the profile size dispersion (i.e. local homogeneity of subgrain and grain structure) on the area of observation window (475 μm^2 in as-pressed specimens and about 12 400 μm^2 in the remaining cases) are presented in Table 5. Extremely high values are found in the as-pressed specimens (note that CV *a* in relatively homogeneous grain systems should not exceed the value of 1) at all values of the lower bound of misorientation Δ and they systematically increase with growing Δ, perhaps as a consequence of vanishing small subgrains (the results obtained at $N = 1$ are not reliable because the observing window is too small). The values of CV *a* after annealing are not shown, because both the annealing times at both the temperatures produce similar grain profile dispersions with CV $a \approx 2$. Further, there is not a systematic dependence of CV *a* after creep on the number of passes but the dispersion of grain profiles is slightly more homogeneous than that one of subgrains, in particular at $N \geq 8$ at 473 K and at an arbitrary *N* at 573 K. The comparison of these results with those ones obtained in aluminum (see [3]) shows, that the dispersion of grain and subgrain profiles in copper is in all examined situations nearly twice as high (as measured by the values of CV *a*).

Table 5 Values of CV *a* in as-pressed specimens and after creep.

	CV *a* in as-pressed Cu				**CV *a* after creep (573 K, 50 MPa)**				
$\Delta \geq$	***N***				***N***				
	1	**2**	**4**	**8**	**1**	**2**	**4**	**8**	**12**
2^o	10	8.3	3.7	1.5-	4.1	5.5	5.8	5.4	5.8
5^o	3.6	11.8	15.1	2.3	3.3	2.4	3.5	4.7	3.6
10^o	3.2	16.6	18.7	6.2	3.4	2.4	3.6	4.7	3.7
15^o	3.2	16.5	18.5	8.3	3.7	2.4	3.6	4.7	3.8

4. Creep and Monkman-Grant relation

The observed minimum creep rates $\dot{\varepsilon}_{min}$ and the times to fracture t_f in aluminum and copper produced by ECAP with different number of passes have already been published (e.g. [7, 13, 17]). They cover the interval between 10^{-8} and 10^{-5} s^{-1} and take from 10^0 to 10^3 hours. Surprisingly accurately they also fulfill the well-known Monkman-Grant relation

$$(\dot{\varepsilon}_{min})^m \cdot t_f = M$$

with the nearly identical values of the constants. The linear regression plots

$$m \log \dot{\varepsilon}_{min} + \log t_f = \log M$$

are shown in Fig. 5. Aluminum data (59 specimens) includes also the specimens with ECAP technology different from B_C, namely A (no specimen rotation after each pass) and C (the rotation by 180^o after each pass). In the case of copper (24 specimens), also the results obtained by creep of the original coarse-grained material (10 specimens) were analyzed. The estimates of the values of *m* and log *M* were obtained by linear regression (see Table 7).

The product $\dot{\varepsilon}_{\min} \cdot t_f$ is usually called the Monkman-Grant (M-G) ductility; it is necessarily lower than the final ductility, which typically ranged between 30 and 50% in creep tests of copper after ECAP (about 15% in the coarse-grained copper) and was higher by about 10 – 20% in aluminum.

Table 7 Results of the regression analysis.

	Al(ECAP)	**Cu(ECAP)**	**Cu(*N*=0)**
m	-0.861	-0.907	-0.896
log *M*	0.162	-0.241	-0.918
mean G-M ductility	0.265	0.162	0.0299
its standard deviation	0.100	0.0720	0.0177

Usually it is expected that the value of *m* is between 0.85 and 1, its rather low value in the case of aluminum is compensated by a positive value of log *M*.

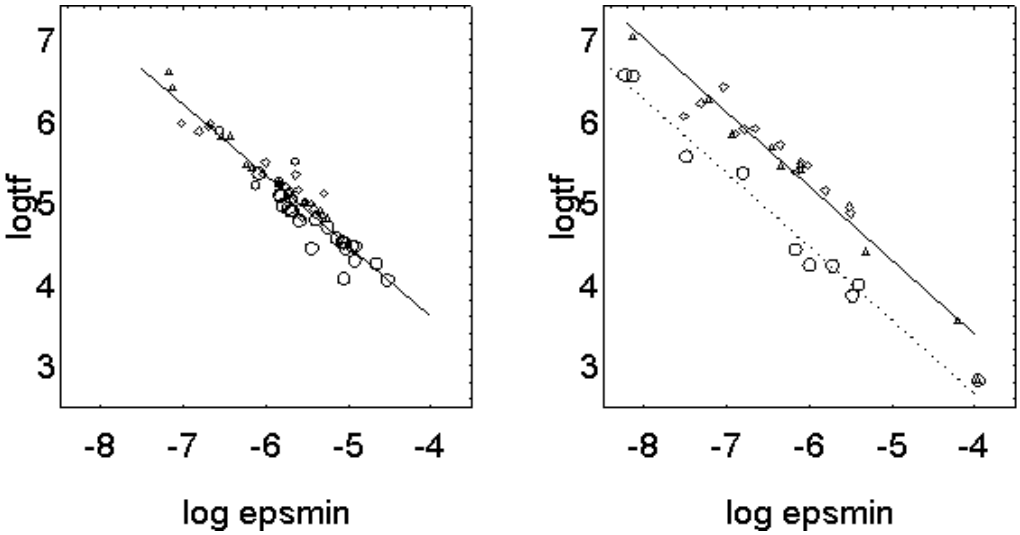

Fig. 5 Monkman-Grant relation for Al (left) and Cu (right): aluminum at 473 K, 15 MPa: △ – route A, ◇ – route B_C, – ❍ route C, 20 MPa: ❍ – route B_C; copper, 80 MPa, route B_C : ◇ – 473 K, △ – 573 K, ❍ – original coarse-grained Cu, 473 K and 573 K. Parameters of the regression lines are in the Table 7.

The comparison of the both diagrams confirm the general approximate validity of the Monkman-Grant relation, which in the present case describes very similarly the creep resistance of the both materials after ECAP as well as also that one of the coarse grained copper. In this connection a considerable difference in the homological temperatures T_{hom} of the both materials should be recalled: for copper at 473 K and 573 K are the values of T_{hom} = 0.55 and 0.62, respectively, whereas for aluminum at 473 K is the value T_{hom} = 0.8. Hence, the validity of the Monkman-Grant relation with the very similar value of *m* is weakened neither by difference in examined materials nor in their homological temperatures. However, a distinct shift occurs in the same material - copper - as a consequence of different final creep ductility.

4. Concluding discussion

Perhaps the most interesting feature of copper subgrain and grain structures after ECAP is the deficit of small angle boundaries with Δ from the interval [5^o, 15^o). They are nearly completely missing in the annealed as-pressed specimens and only rarely reach 10 %. The contribution of subboundaries with $\Delta < 5^o$ never attain the 30 % level, the grain structures look unstable and are inhomogeneous (with high CV a values even after 12 passes and creep at 573 K).

The completely different behavior was observed in aluminum: the proportion of high angle boundaries grew continually with the number N in as-pressed specimens as well as after their annealing during creep tests. Moreover, relatively homogeneous structures (CV $a \approx 2$) formed after higher N and creep. The contribution of subgrains with $\Delta \in [5^o, 15^o)$ systematically exceeded that one of low angle ($\Delta < 5^o$) at $N \geq 4$ (see [10-13]). Even when small subgrains and grains scattered within larger grains and subgrains were also observed in Al, they were less numerous and less stable than in Cu and rather exceptional after creep.

A detailed discussion concerning the effect of ECAP pressing on the creep properties is in [17] and it is only shortly summarized here. The lack of high-angle boundaries can be the reason of high creep resistance after the first pass. The gradual development of such boundaries during subsequent passes makes the dislocation movement easier, the creep rate increases and approximately constant ultimate elongation is attained in a shorter time.
However, such an explanation is unacceptable in the case of copper, where the high angle boundaries are present in reasonable amount even at low number of passes. Nevertheless, certain grain growth also proceeds in copper; it seems that the number of small particle-like grains decreases and at least certain of them transform into larger grains thus promoting the creep by the dislocation motion. The difference in the homological temperatures of copper and aluminum can also influence the creep behavior as well as the structure development. In any case, it seems that a more detailed examination of copper grain structures after ECAP and creep is necessary in order to explain reliably their creep properties.

Acknowledgements

The authors acknowledge the financial support for this work provided by the GA ČR (grant 201/06/0302), by the grant MSM 0021620839 and by the Academy of Sciences of the Czech Republic, Institutional Research Plans No. AV0Z10190503 and AV0Z20410507.

References

[1] M. Furukawa, Z. Horita, M. Nemoto, T.G. Langdon: Processing of Metals by Equal-Channel Angular Pressing, J Mater Sci 36 (2001) 2835-2843

[2] R.Z. Valiev, T.G. Langdon, Principles of equal-channel angular pressing as a processing tool for grain refinement, Progr Mater Sci 51 (2006) 881-981

[3] Y. Estrin, R.J.Hellmig, H.S. Kim, Strength and ductility of ultrafine grained copper: modelling and experiment, Journal of Metastable and Nanocrystalline 17 (2003) 29-36

[4] K.P. Grabovetskaya, K.V. Ivanov, Y.R. Kolobov, Creep Features of Nanostructural Materials Produced by Severe Plastic Deformation, Ann Chim Sci Mater 27 (2002) 89-98

[5] O. Srba, M. Janeček, J. Čížek, M. Dopita, R. Král: Mechanical Properties of Ultrafine-grained Cu Processed by ECAP. WDS'08 Proceedings of Contributed Papers, Part III, Matfyzpress, Praha 2008, 130-135

[6] W. Blum, Y.J. Li, Influence of grain boundaries on steady-state deformation resistance of ultrafine-grained Cu, Phys Stat Sol (a) 201 (2004) 2915-2921

[7] V. Sklenička, J. Dvořák, P. Král, Z. Stonawská, M. Svoboda, Creep processes in pure aluminium processed by equal-channel angular pressing, Mater Sci Eng A 410-411 (2005) 408-412

[8] Y.J. Li, R.Z. Valiev, W. Blum, Deformation kinetics of ultrafine-grained Cu and Ti, Mater Sci Eng A 410-411 (2005) 451-456

[9] C. Xu, T.G. Langdon, Creep and superplasticity in a spray-cast aluminum alloy processed by ECA pressing, Mater Sci Eng A 410-411 (2005) 398-401

[10] L. Ilucová, I. Saxl, M. Svoboda, V. Sklenička, P. Král, Structure of ECAP Aluminium after different number of passes, Image Analysis and Stereology 26 (2007) 37-43

[11] I. Saxl, L. Ilucová, M. Svoboda, V. Sklenička, V.I. Betekhtin, A.G. Kadomtsev, P. Král, Structural Non-homogeneity and Thermal Instability of ECAP Aluminium, Mater Sci Forum 567-568 (2008) 193-196

[12] I. Saxl, V. Sklenička, L. Ilucová, M. Svoboda, P. Král, Subgrain boundaries in ECAP aluminium. Mat Sci Forum 561-565 (2007) 813-816

[13] I. Saxl, V. Sklenička, L. Ilucová, M. Svoboda, J. Dvořák, P. Král, The link between microstructure and creep in ECAP aluminum, Mater Sci Eng A 503 (2009) 82-85

[14] V. Sklenička, J. Dvořák, M. Kvapilová, M. Svoboda, P. Král, I. Saxl, Z. Horita, Effect of Equal-Channel Angular Pressing (ECAP) on Creep in Aluminium Alloys, Mat Sci Forum 539-543 (2007) 2904-2909

[15] P. Král, J. Dvořák, V. Sklenička, Microstructural Evolution and Creep of an Al-0.2wt.%Sc Alloy after Equal-Channel Angular Pressing. Mater Sci Forum 584-586 (2008) 846-851

[16] V. Sklenička, J. Dvořák, P. Král, M. Svoboda, I. Saxl, Some factors affecting the creep behaviour of metallic materials processed by equal-channel angular pressing, presented at 11th Int. Symposium on physics of materials, Prague 24. 8. – 28. 8. 2008 (in press)

[17] I. Saxl, V. Sklenička, Interpretation of Profile and Intercept Counts in Microstructure Characterization, Mater Sci Forum 604-605 (2009) 403-410